DYNAMICS OF MECHANICALLY AND ELECTROSTATICALLY COUPLED MICROCANTILEVERS

Mariateresa Napoli   Wenhua Zhang   Kimberly Turner   Bassam Bamieh

Department of Mechanical Engineering,
University of California,
Santa Barbara, CA 93106, U.S.A.
{*napoli,whzh,turner,bamieh*}*@engineering.ucsb.edu*

Abstract— **In this paper we study the behavior of a pair of electrostatically and mechanically coupled microcantilevers. For the case of cantilevers excited by a periodic voltage, we show that the underlying linearized dynamics are governed by a pair of *coupled Mathieu* equations. We provide experimental evidence that confirms the validity of the mathematical model proposed, including in particular a mapping of the first order *coupled parametric resonance* region. The mechanical coupling coefficients are identified from experimental data, and their values are shown to match well those obtained by finite element methods.**

I. INTRODUCTION

In recent years the trend towards miniaturization of electro-mechanical devices has been accompanied by a widespread interest in array architectures. Examples of such devices can be found in data storage and retrieval applications [1], biosensors [2], and multi-probe scanning devices [3] to cite but a few.

Currently, these multi-probe devices are designed with large spacing between the individual elements. This essentially decouples the dynamics of the individual probes, that can be considered to behave as isolated units. The drawback of this configuration is, of course, a decrease in the potential throughput of the system.

The device that we consider in this paper consists of a pair of closely spaced microcantilevers. The extension to the case of an array of tightly packed cantilevers is not conceptually difficult and is obtained as a generalization of the analysis we present here. In our design each microcantilever constitutes the movable plate of a capacitor and its displacement is controlled by the voltage applied across the plates. Cantilever geometries are particularly interesting, due to their wide range of applications, including small force detection [4], [5], AFM, mechanical filters for telecommunication [6], and chemical sensor arrays [7].

We present a mathematical model that explicitly incorporates the dynamical coupling between the microcantilevers. Using simple parallel plate theory and for the common case of sinusoidal forcing, we have demonstrated [8] that the dynamics of each isolated cantilever are governed by a Mathieu equation. Here we show that the close spacing and the fact that the cantilevers are connected to a common base introduces a coupling in their dynamics, which is both electrostatic and mechanical. In particular, we show that the system is governed by a pair of *coupled Mathieu* equations. We produce experimental evidence that validates the mathematical model proposed, including a mapping of the first instability region of the Mathieu equation. The natural frequency of each isolated beam and the electrical and mechanical coupling coefficients are determined from the identification of the experimental data. These results are also validated by Finite Element simulation methods.

The paper is organized as follows: In Section 2 we develop the mathematical model of the electrostatically actuated cantilever pair. In Section 3 we present the experimental results that validate the model including, in particular, the mapping of the first instability region of the coupled Mathieu equation. Finally, we present our conclusions in Section 4.

II. MODEL DESCRIPTION

Figure (1) shows the geometry of our device. It consists of two microbeams connected to the same base, each forming a micro-capacitor, with the second (rigid) plate placed underneath the (movable) cantilever visible in the picture. The vertical displacement of each cantilever can be controlled by applying a voltage across the plates. Though each cantilever is independently actuated, its dynamics are influenced by the presence of the other cantilever. More precisely, the coupling is both mechanical, because the microbeams are connected to the same base, and electrical, due to the fringing fields generated by the capacitor nearby.

The force acting on each microbeam can be split into several components. By using simple parallel plate theory, the linearized electrostatic attractive force between the capacitor plates of the i-th cantilever, $i = 1, 2$, can be expressed as

$$F_{a,i} = \frac{\epsilon_o A}{2d^2}(1 + 2\frac{z_i}{d})V_i^2$$

where d is the gap between the electrodes, A is the area of the capacitor plates, and V_i is the voltage applied.

The mechanical coupling force $F_{mech,i}$ has been modeled as a spring like force, proportional to the difference in the
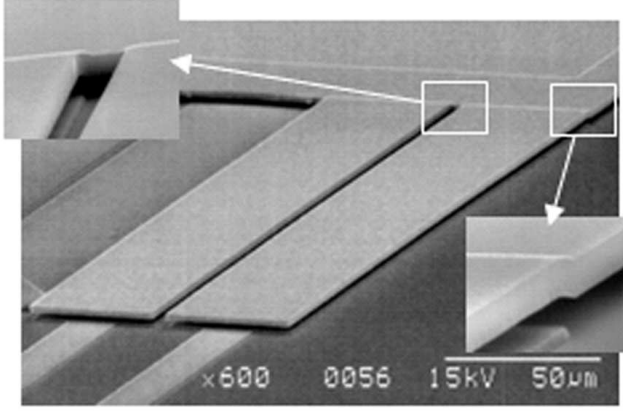
Fig. 1. SEM micrograph of the device. The insets show details of the mechanical connection to the base and between the cantilevers.

vertical displacement z_i of the cantilevers,

$$F_{mech,i} = \gamma(z_i - z_j).$$

Due to the symmetry of the device, the coefficient of mechanical coupling γ is the same for both cantilevers.

As far as the electrostatic coupling is concerned, we consider that the voltage applied to each capacitor results in a charge induced on each cantilever, that can be expressed as

$$q_1 = c_{1,1}V_1 + c_{1,2}V_2,$$
$$q_2 = c_{2,1}V_1 + c_{2,2}V_2.$$

The interaction between these induced charges is described via a point charge model. The idea is shown schematically in Figure (2). Each cantilever is represented as a charged particle,
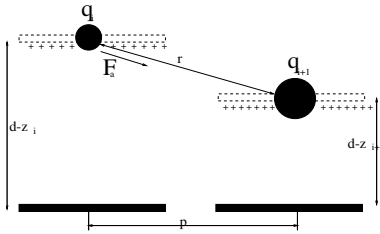

Fig. 2. A schematic of the coupling capacitance model.

q_i, and the mutual interaction is described by Coulomb's law

$$F_{elec,i} = \frac{1}{4\pi\epsilon_o} \frac{q_i q_j}{r^2}.$$

We assume that the lateral stiffness of the cantilevers is large enough to prevent any lateral motion, so that the only component of the force that really affects their behavior is the vertical, whose first order approximation is

$$F_{elec,i}^{\perp} = [K_{ii}V_i^2 + K_{i,j}V_iV_j + K_{j,j}V_j^2](z_i - z_j).$$

Taking into account all these components, the linearized equation of motion for the vertical displacement of each

cantilever can be written as

$$\ddot{z}_i + \nu_i\dot{z}_i + \omega_{ri}^2 z_i = F_{a,i} + F_{mech,i} + F_{elec,i}^{\perp} \quad (1)$$

where ν_i and ω_{ri} are respectively the normalized damping coefficient and the natural resonant frequency of the i-th cantilever.

For the special case of $V_i = V_{oi}\cos\omega t$, Eq. (1) can be rewritten as

$$\ddot{z}_i + \nu_i\dot{z}_i + [a_i + \epsilon_i\cos 2\omega t]z_i + [b_1 + b_2\cos 2\omega t]z_j = $$
$$K_e d(V_{oi}\cos\omega t)^2, \quad (2)$$

where $a_i = \omega_{ri}^2 - \gamma/m - (K_eV_{oi}^2 + K_T)$, $\epsilon_i = -(K_eV_{oi}^2 + K_T)$, $b_1 = \gamma/m + K_T$, $b_2 = K_T$, $K_T = (K_{11}V_{o1}^2 + K_{12}V_{o1}V_{o2} + K_{22}V_{o2}^2)/(2m)$ and $K_e = \epsilon_o A/(md^3)$.

Eq. (2) represents a system of periodic differential equations, which we refer to as *coupled Mathieu equations*, since their algebraic structure is reminiscent of the famous Mathieu equation. In the absence of coupling, they reduce to a standard Mathieu equation, which indeed describes the dynamics of an isolated beam [8]. In the next section we will provide experimental data to validate the model proposed and demonstrate how the coupling, often considered a drawback, can instead be advantageously exploited from an engineering point of view.

III. EXPERIMENTAL VALIDATION OF THE MODEL

The device we have used in our experimental setup consisted of two $200\mu m \times 50\mu m \times 2\mu m$ highly doped polysilicon cantilevers, fabricated using the MUMPS/CRONOS process, with a gap between the electrodes of about $2\mu m$ and separated by a distance of $5\mu m$ (see Figure(1)). The mechanical response of the cantilevers was tested in vacuum ($p = 8mT$), using laser vibrometry [9] to measure displacement and velocity near the free end of each cantilever, when electrostatically driven with different AC voltage signals.

Figure (3) represents the measurement of the frequency responses of the system subject to small excitations. In this case, the time-varying coefficients in eq. (2) can be neglected and the device is described by a system of second order ordinary differential equations. By Gij we denote the transfer function from the voltage input applied to the j-th cantilever to the velocity output measured on the i-th cantilever, when the other voltage input is set to zero. Notice the presence of two peaks in the transfer function of each single cantilever, a consequence of coupling. The analytical expression of these transfer functions is given by

$$G_{ii} = \frac{K_e d(s^2 + \nu_i s + \omega_{ri}^2 - \Gamma + K_{ii}V_{oi}^2)}{(s^2 + \nu_i s + \omega_{ri}^2 - \Gamma - (K_e - K_{ii})V_{oi}^2)(s^2 + \nu_j s + \omega_{rj} - \Gamma + K_{ii}V_{oi}^2) - (\Gamma - K_{ii}V_{oi}^2)^2},$$

$$G_{ij} = -\frac{K_e d(\Gamma - K_{ii}V_{oi}^2)}{(s^2 + \nu_i s + \omega_{ri}^2 - \Gamma - (K_e - K_{ii})V_{oi}^2)(s^2 + \nu_j s + \omega_{rj} - \Gamma + K_{ii}V_{oi}^2) - (\Gamma - K_{ii}V_{oi}^2)^2},$$

By fitting the data to this model, as shown in Figure (3), we get that the resonant frequencies of the isolated beams are respectively $\omega_{r1} = 48870Hz$ and $\omega_{r2} = 51520Hz$, while the damping coefficients turn out to be $Q_1 = Q_2 \approx 3000$. The difference in the values of ω_{r1} and ω_{r2}, in spite of the

TRANSDUCERS '03
The 12th International Conference on Solid State Sensors, Actuators and Microsystems, Boston, June 8-12, 2003
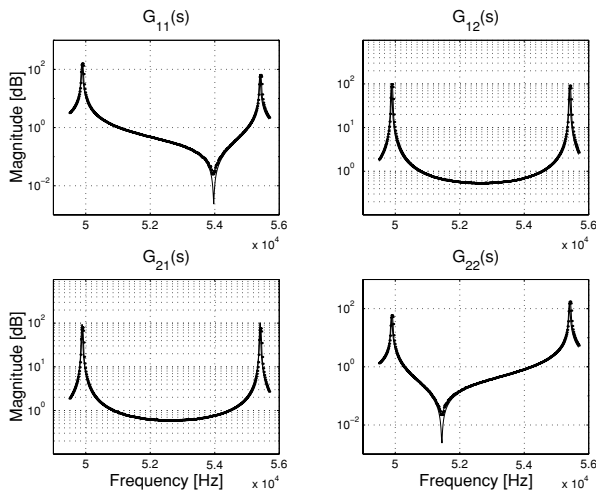
1089

Fig. 3. Magnitude of the frequency responses of the coupled cantilevers with different input/output combinations. The dotted (blue) line represents experimental data; the solid (red) line the fitted data.

Fig. 4. Experimental estimation of the electrostatic coefficients. K_{ij} are the coefficients of the electrostatic coupling force, $F_{elec,i}$; K_e is the coefficient of the attractive force, $F_{a,i}$, between the cantilever and its ground plate.

fact that the beams have the same geometry and material, is to be attributed to the different configuration of the anchor, which has an overhang in correspondence to one of the beams. The coefficient of mechanical coupling $\Gamma = \gamma/m$ has been estimated by fitting the Power Spectral Density (PSD) of the vibrations induced by thermal noise, in order to eliminate the electrostatic coupling and isolate its contribution. The following table presents the value of some significant parameters obtained by identification and compares it with the value obtained by finite element methods.

	ω_1	ω_2	ω_{r1}	ω_{r2}	Γ
FEM	50045	55868	48830	51681	$1.10e^{10}$
Testing	48896	55417	48870	51520	$1.02e^{10}$
Error	2.3%	0.8%	0.1%	0.3%	7.8%

Notice that the presence of the zero in the transfer functions G_{11} and G_{22} is determined by the mechanical and electrostatic coupling, and its location changes with the amplitude of the driving voltage. This gave us a way to estimate the values of the electrostatic coefficients K_{11} and K_{22}, as shown in Figure (4 (a) and (b)). Similarly, the coefficient K_e was estimated from the shift in the poles with the applied AC voltage. Finally, the coefficient K_{12} was estimated by applying the same voltage to both inputs and considering the transfer function $\bar{G}_{11}$. It is not diffcult to see that its numerator is given by

$$K_e d(s^2 + \nu_2 s + \omega_{r2}^2 - 2\Gamma - K_e V_o^2 + 2K_T),$$

and that therefore also in this case the zero location is related to the changes with the amplitude of the AC voltage applied, V_o.

It is worth noting that the equivalent stiffnesses corresponding to these coupling parameters are of the same order as the mechanical stiffness of the uncoupled cantilever, indicating significant coupling in this system.

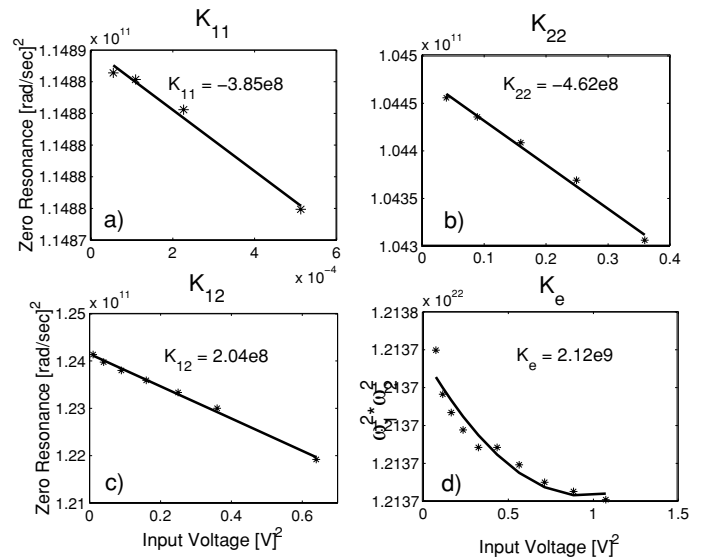As the amplitude of the driving signal increases, so do the

values of ϵ_i and b_2 and this linear time-invariant approximation of the system is no longer appropriate. In order to predict and explain the rich dynamics that the system shows, we have to return to the original equations (2).

A. Parametric Resonance

Parametric resonance is a form of mechanical amplification, in which large responses can be generated even if the excitation frequency is far away from the system's natural frequency. This pheomenon is a characteristic of systems, called *parametrically excited*, in which the input appears as a time-dependent coefficient, as in eq. (2).

In [8] we demonstrated that an electrostatically actuated microcantilever can exhibit parametric resonance. We illustrated the relation between the driving frequencies that induce parametric amplification and the natural resonant frequency of the device [10], [11]. We also provided a mapping of the first region of parametric amplification.

Figure (5) shows the experimental mapping of this region for a pair of cantilevers. During these experiments one of the inputs is set to zero, while the other is set to $V_i = \frac{V_o}{2}\sqrt{1 + \cos \omega_o t}$. Which input is selected is in fact inconsequential, given the symmetry of the device, and the results can be reproduced using either one of them. Note that in this case the parametric resonant region is composed of three branches, that correspond to the driving frequency being equal to $a) 2\omega_1$, $b) 2\omega_2$, and $c) \omega_1 + \omega_2$, where ω_i denotes the value of either one of the resonant peaks in the frequency responses of Figure(3).

During the parametric amplification regime the beams exhibit an oscillation that is bounded by the system nonlinearities [11]. Indeed for large oscillation amplitudes, both the linear spring model and the electrostatic force previously introduced need to be corrected by adding cubic terms [12]. Hence, eq.

TRANSDUCERS '03
The 12th International Conference on Solid State Sensors, Actuators and Microsystems, Boston, June 8-12, 2003
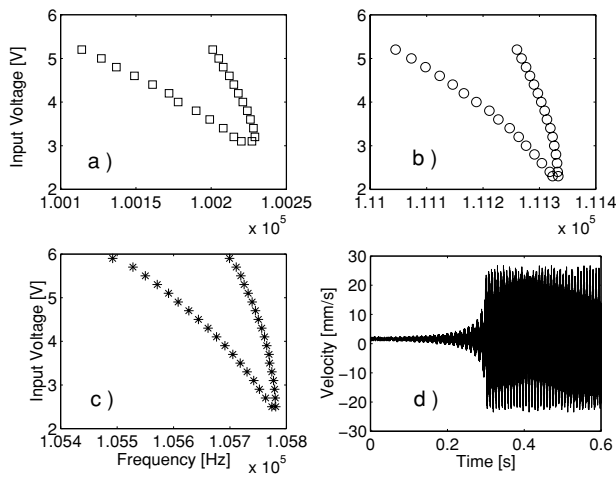
1090

Fig. 5. First region of coupled parametric amplification, with the electric signal applied to one cantilever only. The three tongues correspond respectively to a) $2w_1$; b) $2w_2$; c) $w_1 + w_2$. w_1 and w_2 correspond to the two peaks of the transfer functions as shown in Figure 3. Picture d) shows the exponential growth of the output inside the region of parametric amplification.

(2) becomes

$$\ddot{z}_i + \nu_i \dot{z}_i + [a_i + \epsilon_i \cos 2\omega t]z_i + a_{i3}z_i^3 + $$
$$[b_1 + b_2 \cos 2\omega t]z_j = K_e d(V_{oi} \cos \omega t)^2, \quad (3)$$

where a_{i3} denotes the effective cubic stiffness of the beam, which includes both electrostatic and structural contributions. What we observe when driving the cantilever in parametric resonance regime is : in case $a)$ and $b)$ a subharmonic $2:1$ oscillation at half the frequency of excitation; in case $c)$ an oscillation having both components. Note also that during the transition from non-parametric to parametric region, the response shows, as expected, a characteristic exponential growth (see Figure 5d)). Finally, the effect of damping is again in the upward shift of the tongues in the V_o-ω_o parameter space, so that the tip of the tongues do not start on the horizontal axis.

IV. CONCLUSIONS

In this paper we have presented a mathematical model for a pair of electrostatically actuated microcantilevers, which explicitly incorporates their dynamical coupling. In our design the cantilevers, which are connected to a common base, constitute the movable plate of micro-capacitors and their displacement is independently controlled by the voltage applied across the plates. In the case of sinusoidal excitation, we have proved that their dynamics are regulated by a pair of *coupled Mathieu* equations. We have provided experimental validation of the mathematical model, including a mapping of the first region of parametric amplification. From this work, many sensing applications can be realized, utilizing the sharp transitions from non-resonant to resonant state, which are present in the parametrically resonant state. Filters and sensors using this mechanism are being explored. In addition, an extension to multi-cantilever arrays is also being investigated. This result offers designers tangible guidelines needed to implement novel parametric devices.

REFERENCES

[1] M. Despont et al., "VLSI-NEMS Chip for Parallel AFM Data Storage", in *Sensors and Actuators*, 80 (2000) 100-107.
[2] C.L. Britton et al., "Multiple-Input Microcantilever Sensors", in *Ultramicroscopy*, 82 (2000) 17-21.
[3] P. Indermhule et. al., "Fabrication and Characterization of Cantilevers with Integrated Sharp Tips and Piezoelectric Elements for Actuation and Detection for Parallel AFM Applications", in *Sensors and Actuators A*, 60 (1997) 186-190.
[4] D. Rugar, et. al., "Mechanical parametric amplification and thermomechanical noise squeezing", *Physical Review Letters*, 67 (6), pp. 699-702.
[5] "Nanometer-scale force sensing with MEMS devices", *IEEE Sensors Journal*, 1 (2), pp. 148-157, 2001.
[6] C. T.-C. Nguyen et. al., "Design and performance of CMOS micromechanical resonator oscillators", in *IEEE Proceedings 1994 International Frequency Control Symposium*, pp. 127-134, 1994.
[7] T. Thundat, et. al., "Microcantilever sensors", *Microscale Thermophysical engineering*, 1, pp. 185-199, 1997.
[8] M. Napoli, R. Baskaran, K. Turner, B. Bamieh, " Understanding Mechanical Domain Parametric Resonance in Microcantilevers", in *Proc. of the IEEE 16th Annual Int. Conf. on MEMS*, 19-23 Jan. 2003, Kyoto JP, pp.169-172.
[9] K. Turner, "Multi-Dimensional MEMS Motion Characterization using Laser Vibrometry", in *Digest of Technical Papers Transducers '99*, 10th Int. Conf. on Solid-State Sensors and Actuators, Sendai, Japan 1999.
[10] K. Turner et al., "Five Parametric Resonances in a MicroElectroMechanical System", in *Nature*, 396, pp.149-156, 1998.
[11] R. Rand, "Lecture Notes on Nonlinear Vibrations", available online at *http://www.tam.cornell.edu/randdocs/*.
[12] W. Zhang et. al., "Effect of cubic nonlinearity on auto-parametrically amplified resonant MEMS mass sensor", *Sensors & Actuators A*, 3578, pp. 1-11, 2002.

TRANSDUCERS '03
The 12th International Conference on Solid State Sensors, Actuators and Microsystems, Boston, June 8-12, 2003

1091